

Perpendicular magnetic anisotropy and strong magneto-optic properties of SrRuO₃ epitaxial films

L. Klein,^{a)} J. S. Dodge, T. H. Geballe, and A. Kapitulnik
Edward L. Ginzton Laboratory, Stanford University, Stanford, California 94305

A. F. Marshall
Center for Materials Research, Stanford University, Stanford, California 94305

L. Antognazza and K. Char
Conductus Inc., Sunnyvale, California 94086

(Received 27 October 1994; accepted for publication 7 March 1995)

Epitaxial films of the ferromagnetic perovskite SrRuO₃ were measured with a bulk magnetometer and with a local magneto-optic Sagnac interferometer in transmission and in reflection. We find a magnetic easy axis perpendicular to the films, and for saturated remanent magnetization along this direction the Faraday rotation and the Kerr rotation at $\lambda=840$ nm are about 0.75×10^5 deg/cm and 0.85° , respectively. The temperature dependence of the remanent magnetization in the low temperature limit is dominated by spin-wave excitations, yielding a notable decrease with $T^{3/2}$. Using Sagnac-Kerr scanning and transmission electron microscopy imaging we correlate the coercivity with the grain size. © 1995 American Institute of Physics.

SrRuO₃ is an intriguing material as a rare case of 4*d* itinerant ferromagnetism. Extensive measurements¹⁻³ of polycrystalline samples and single crystals of SrRuO₃ have revealed high magnetocrystalline anisotropy, complex domain structure, and a large difference between the high-temperature Curie-Weiss magnetic moment and the low temperature saturation magnetization, $2.56 \mu_B/\text{Ru}$ and $1.1 \mu_B/\text{Ru}$, respectively. The discovery of the perovskite high temperature superconductors (HTS) has intensified the interest in SrRuO₃, for films of this compound can be successfully epitaxially grown on top of HTS films.⁴⁻⁶ SrRuO₃ films have been used so far for basic studies of Josephson junctions with ferromagnetic barriers, YBa₂Cu₃O₇-SrRuO₃-YBa₂Cu₃O₇,⁶ and they have been proposed as potentially useful elements in magneto-optic and electro-optic devices. However, to date very little is known of the magnetic properties which distinguish films from single crystals, and of the magneto-optic characteristics which are particularly important for thin film applications.

In this letter, we report measurements on epitaxial films of SrRuO₃: 1000 Å thick (S1) and 3000 Å thick (S2) films on LaAlO₃ substrates, and a 1000 Å thick film (S3) on a SrTiO₃ substrate. Samples S1 and S3 were prepared in the same deposition. SrRuO₃ is a pseudocubic perovskite with a lattice constant of 3.96 Å. The films are oriented with the [100] direction (in the cubic system) perpendicular to the plane of the film, and their T_c is about 144 K. The actual structure of SrRuO₃ is orthorhombic and the *c* axis lies in the plane of the film. The orientation of the films and their Curie temperature are consistent with a previous report on films.⁴ The magnetic measurements were done with a quantum design superconducting quantum interference device (SQUID). The optical measurements were done with a state-of-the-art Sagnac interferometer, which operates with a superluminescent diode source at $\lambda=840$ nm. The Sagnac interferometer can be used in transmission for Faraday rotation

measurements, or in reflection for Kerr rotation measurements. A full description of this apparatus in its various configurations has been given elsewhere.⁷ Here we stress the immunity of our apparatus to polarization changes due to reciprocal effects (such as linear birefringence), and the achieved sensitivity of $1 \mu\text{rad}/\sqrt{\text{Hz}}$ for rotation angle without drift.

For saturated remanent magnetization M_0 perpendicular to the film, the Faraday measurements at $\lambda=840$ nm yield a rotation of about 0.75×10^5 deg/cm. In the Kerr configuration at normal incidence we find a rotation of about 0.85° for S2, which is 3000 Å thick, and about 0.55° in S1 and S3, which are both 1000 Å thick. These values of the Faraday and Kerr rotations are within an order of magnitude of the values for the 3*d* ferromagnetic elements, iron, nickel, and cobalt, which are among the most strongly magneto-optically active materials known. The Faraday rotation (as well as the Kerr rotation) of ferromagnets is proportional to M_0 and the spin-orbit coupling.⁸ Ruthenium has a spin-orbit coupling of about $900 \text{ (cm}^{-1}\text{)}$, compared to $400 \text{ (cm}^{-1}\text{)}$ for iron,⁹ and M_0 of SrRuO₃ and Fe are 2 and 21.8 kOe, respectively. Assuming the same proportionality for iron and ruthenium, the estimated Faraday rotation for SrRuO₃ is about 1×10^5 deg/cm, which is in very good agreement with the experimental data. This observation implies that the spin-orbit coupling of ruthenium is the source of the large magneto-optic parameters; consequently, large magneto-optic constants should be anticipated in other materials which include magnetic ions of ruthenium. Even larger magneto-optic constants might be possible in ferromagnets containing 5*d* elements such as Ir.

Figure 1 shows the reduced perpendicular remanent magnetization M/M_0 of S1 and S3 as a function of the reduced temperature T/T_c ($T_c=144$ K), where M_0 for both samples corresponds to about $1.1 \mu_B$ per Ruthenium atom, consistent with previous reports.^{2,6} In addition, the figure shows, for comparison, the mean field curve for spin $S=1$. The magnetization of S1 and S3 was measured in the low

^{a)}Electronic mail: klein@loki.stanford.edu

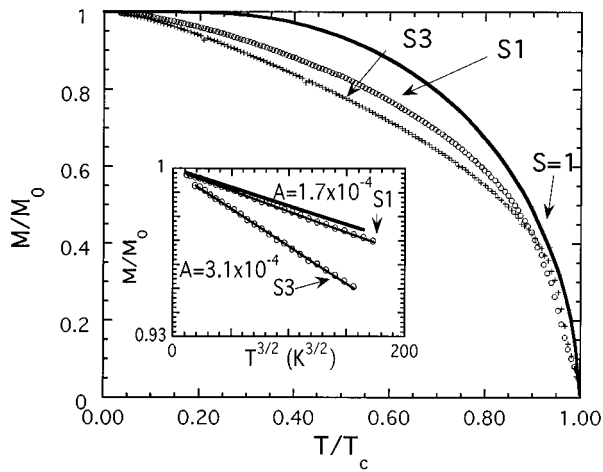


FIG. 1. The reduced remanent magnetization of S1 (1000 Å on LaAlO₃) and S3 (1000 Å on SrTiO₃) as a function of the reduced temperature. The mean field solution with $J=1$ is given for comparison. Inset: The reduced remanent magnetization (after correcting for the T^2 term) as a function of $T^{3/2}$ with a fit to the spin wave correction $M(T)/M_0=1-AT^{3/2}$. The thick solid line is the theoretical prediction assuming $S=1$, with no adjustable parameters, which yields $A=1.6\times 10^{-4}$ ($1/K^{3/2}$).

temperature interval of $5\text{ K} < T < 70\text{ K}$ upon warming and cooling, and we verified that the change in the magnetization is reversible. It is clear that the notable decrease of the magnetization in the low temperature limit cannot be fit well within the mean field approximation for $S=1$ (or with $S=1/2$ as was suggested previously²). Therefore, there are other contributing factors which suppress the magnetization. The dominant excitations known to suppress the magnetization in the low temperature limit are spin-wave excitations, which according to the Bloch law suppress the magnetization as $M(T)/M_0=1-AT^{3/2}$. In this model $A=c/S(k_B/2JS)^{3/2}$, where $c=0.059$ for a simple cubic magnetic lattice (as it is in our case), S is the total spin of Ru⁴⁺, and $J=26.33\text{ k}_B\text{K}$ is the exchange interaction that may be extracted using the high temperature series expansion result $k_B T_c/J=5(z-1)[11S(S+1)-1]/96$,¹⁰ where z is the number of nearest neighbors. Inserting the known parameters, we find for $S=1$, $A=1.6\times 10^{-4}$ ($1/K^{3/2}$). In itinerant ferromagnets, the low temperature magnetization is further suppressed by a term BT^2 , which is due to Stoner excitations of magnetic electrons. These excitations appear to be predominant for remanent magnetization in the parallel direction (in which, as we discuss below, the remanent magnetization is about half of the perpendicular remanent magnetization) and a T^2 term is found with $B\sim 1.45\times 10^{-5}$ ($1/K^2$). Evidently, in this direction there is a suppression of spin-wave excitations. The inset of Fig. 1 shows the magnetization of S1 and S3 as a function of $T^{3/2}$, where a correcting term of BT^2 was added to each magnetization. The theoretical prediction without any fitting parameters is shown for comparison. We see that the linear fit of the experimental data is remarkable. The fit to $T^{3/2}$ law is clearly observed even without the small T^2 correction, but the prefactors of $T^{3/2}$ are reduced by about 30% with this correction. It seems quite evident that the spin-wave excitations are predominantly responsible for the rapid decrease of the remanent magnetization at low temperatures; however, for a strin-

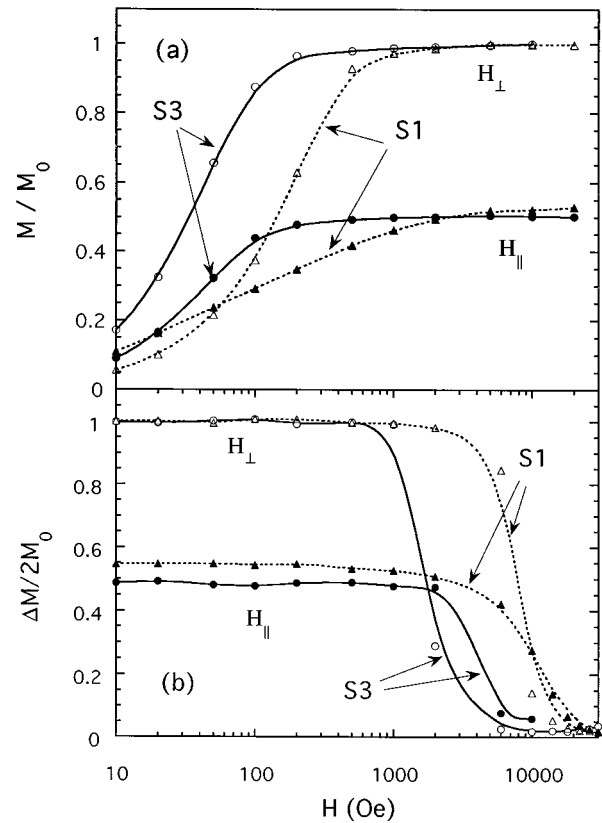


FIG. 2. (a) The reduced remanent magnetization of S1 (1000 Å on LaAlO₃) and S3 (1000 Å on SrTiO₃) at $T=5\text{ K}$ and zero field, as a function of the cooling field parallel and perpendicular to the film. (b) The normalized height of the magnetization loops at $T=5\text{ K}$, as a function of the applied field for S1 and S3. $\Delta M=M(H^-)-M(H^+)$, where $M(H^-)$ and $M(H^+)$ are the magnetizations at the field H in the descending and ascending branches of the hysteresis loop, respectively.

gent estimate of their contribution, an accurate determination of the T^2 correction is needed. We believe that these low temperature excitations are an intrinsic property, and thus should be observed in bulk material as well. Preliminary results on polycrystals of SrRuO₃ support this claim.¹¹

The coercivity of the films depends on the field direction and on sample-specific properties. Figure 2(a) shows the remanent magnetization of S1 and S3 at $T=5\text{ K}$, after cooling in different fields along different directions; Fig. 2(b) shows the height of the hysteresis loops ΔM of the same samples as a function of H , at $T=5\text{ K}$, where ΔM is normalized by $2M_0$. We define $\Delta M=M(H^-)-M(H^+)$, where $M(H^-)$ and $M(H^+)$ are the magnetizations at the field H in the descending and ascending branches of the hysteresis loop, respectively. Both figures demonstrate that the remanent magnetization is maximized only when the field is *perpendicular* to the film; and that the films are less coercive for fields in this direction. TEM micrographs of S1 and S3 show two crystallographic domain structures, which result from two possible orientations of the c axis (of the orthorhombic axes) in the plane of the film, giving 7.86 Å fringes at 90° to each other. Therefore, the observed easy axis is a $[110]$ direction in the orthorhombic coordinate system. The correspondence between the easy axes in films and those observed in single crystals² is not fully clear at this stage and further study is needed. We can however infer from

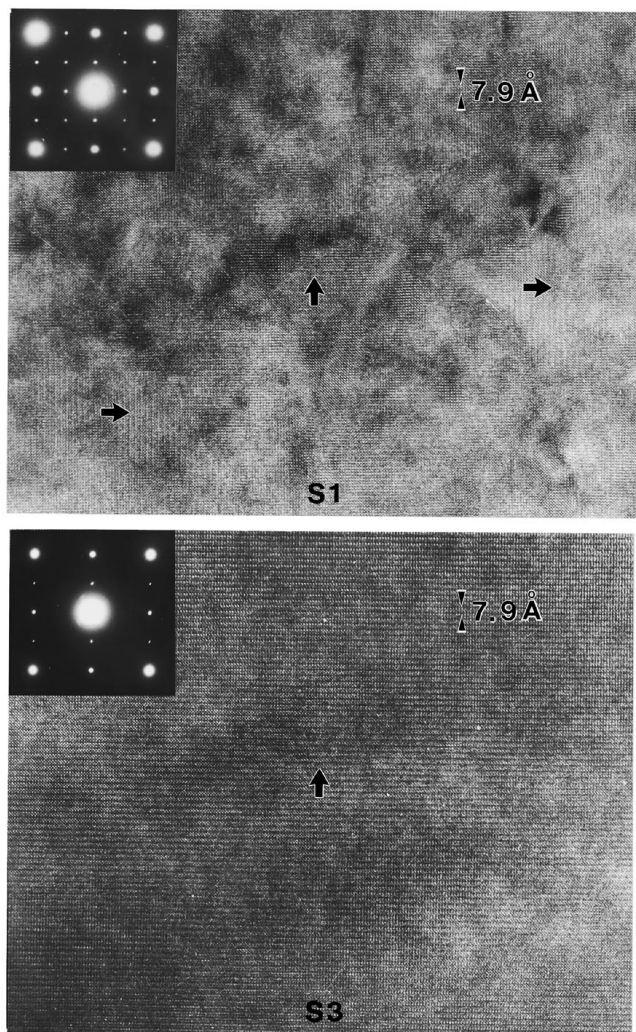


FIG. 3. (Top) Several domains in S1 (1000 Å on LaAlO_3) are indicated by arrows showing the direction of the c axis with 7.9 Å lattice fringe spacing. The selected area diffraction pattern (inset) shows two c -axis orientations. (Bottom) A small area of a single domain in S3 (1000 Å on SrTiO_3). The selected area diffraction pattern (inset) actually comes from an area about 3 μm in diameter and shows a single c -axis orientation.

our observations combined with the magnetocrystalline anisotropy of bulk SrRuO_3 in its pseudo-tetragonal phase² that the two types of grains have a *perpendicular* easy axis, whereas in the plane the easy axis of the two types of grains are at 90° to each other.

In order to elucidate the origin of the different coercive behavior of S1 and S3 we used local optical scanning with the Kerr–Sagnac interferometer, where the spot diameter is about 5 μm . We cooled the samples S1 and S3 in zero field and measured the Kerr rotation at several hundred different locations on each sample. We find that the standard deviation of the rotation for S3 is ten times larger than that of S1. Assuming that the local magnetization is equally distributed among the different orientations of the easy axes, and knowing the rotation at saturation, we can estimate a domain size of ~ 400 Å in S1, and a domain size of ~ 4000 Å in S3. Using both TEM imaging and selected area diffraction techniques we find (see Fig. 3) that the average crystallographic domain size of S1 is consistent with the magnetic domain

size. For S3 the average crystallographic domain size is larger than the magnetic domain size; consequently we infer that the properties of S3 are largely unaffected by granularity. On the other hand the behavior of S1 has characteristics of ferromagnetic fine particles. The critical size for single domain particles is roughly about $[0.4(K/(M_0)^2)] \times [(JS^2\pi^2/Ka)^{0.5}] \sim 2000$ Å, where $K=2$ T (Ref. 2) is the anisotropy energy and a is the magnetic lattice constant.¹² Therefore, it is likely that the crystallographic grains of S1 act as weakly coupled single domain particles. Support for this scenario is given by the different fields needed to saturate the remanent magnetization of S1 and S3 as we cool through the Curie point. In the absence of fine particles, saturation is ensured when $H + 2K/M > H_d = 4\pi M$. On the other hand, in the presence of single domain particles, the applied field should overcome shape anisotropy and thermal fluctuations in order to prevent freezing of single domains in different directions.

In conclusion, we find that SrRuO_3 films have high perpendicular remanent magnetization and large magneto-optic constant. The temperature dependence of the magnetization in the low temperature limit is dominated by spin-wave excitations, and the coercivity is determined by both intrinsic magnetocrystalline anisotropy and the size of the crystallographic grains. The combined magnetic and magneto-optic features make this material interesting for applications, in particular in configurations with HTS films, since in these cases the low Curie temperature is not a drawback. The dominant role of the large spin–orbit coupling in determining the strong magneto-optic properties leads us to infer that using magnetic ions with higher spin–orbit coupling (such as iridium) might enhance these properties still further.

The authors would like to thank C. Herring and J. Snyder for useful discussions. This work has been supported by the Department of Energy Grant No. DE-FG03-94ER-45528. The films were characterized in the Center for Materials Research at Stanford University. One of us (L.K.) would like to thank the support by the Rothschild Fellowship.

- ¹J. M. Longo, P. M. Raccach, and J. B. Goodenough, *J. Appl. Phys.* **39**, 1327 (1968).
- ²A. Kanbayasi, *J. Phys. Soc. Jpn.* **41**, 1876 (1976); *ibid.* **41**, 1879 (1976); *ibid.* **44**, 89 (1978); *ibid.* **44**, 108 (1978).
- ³P. A. Cox, R. G. Egdell, J. B. Goodenough, A. Hamnett, and C. C. Naish, *J. Phys. C* **16**, 6221 (1983).
- ⁴C. B. Eom, R. J. Cava, R. M. Fleming, J. M. Philipps, R. B. van Dover, J. H. Marshall, J. W. P. Hsu, J. J. Krajewski, and W. F. Peck Jr., *Science* **258**, 1766 (1992).
- ⁵X. D. Wu, S. R. Fltyn, R. C. Dye, Y. Coulter, and R. E. Muenchausen, *Appl. Phys. Lett.* **62**, 2434 (1993).
- ⁶L. Antognazza, K. Char, T. H. Geballe, L. L. H. King, and A. W. Sleight, *Appl. Phys. Lett.* **63**, 1005 (1993).
- ⁷S. Spielman, K. Fesler, C. B. Eom, T. H. Geballe, M. M. Fejer, and A. Kapitulnik, *Phys. Rev. Lett.* **65**, 123 (1990); S. Spielman, J. S. Dodge, L. W. Lombardo, C. B. Eom, M. M. Fejer, T. H. Geballe, and A. Kapitulnik, *Phys. Rev. Lett.* **68**, 3472 (1992).
- ⁸P. N. Argvres **97**, 334 (1955).
- ⁹J. S. Griffith, *The Theory of Transition Metal Ions* (Cambridge University Press, Cambridge, 1961), p. 113.
- ¹⁰G. S. Rushbrooke and P. J. Wood, *Mol. Phys.* **1**, 257 (1958).
- ¹¹Snyder (private communication).
- ¹²B. D. Cullity, *Introduction to Magnetic Materials* (Addison-Wesley, Reading, MA, 1972), p. 311.